

ENHANCING PLASTICITY FOR FIRST SESSION ADAPTATION CONTINUAL LEARNING

Imad Eddine Marouf¹Subhankar Roy²Stéphane Lathuilière^{1,3}Enzo Tartaglione¹¹LTCI, Télécom-Paris, Institut Polytechnique de Paris, France²University of Bergamo, Italy³Inria at University Grenoble Alpes, LJK, France

ABSTRACT

The integration of large pre-trained models (PTMs) into Class-Incremental Learning (CIL) has facilitated the development of computationally efficient strategies such as First-Session Adaptation (FSA), which fine-tunes the model solely on the first task while keeping it frozen for subsequent tasks. Although effective in homogeneous task sequences, these approaches struggle when faced with the heterogeneity of real-world task distributions. We introduce Plasticity-Enhanced Test-Time Adaptation in Class-Incremental Learning (PLASTIC), a method that reinstates plasticity in CIL while preserving model stability. PLASTIC leverages Test-Time Adaptation (TTA) by dynamically fine-tuning LayerNorm parameters on unlabeled test data, enabling adaptability to evolving tasks and improving robustness against data corruption. To prevent TTA-induced model divergence and maintain stable learning across tasks, we introduce a teacher-student distillation framework, ensuring that adaptation remains controlled and generalizable. Extensive experiments across multiple benchmarks demonstrate that PLASTIC consistently outperforms both conventional and state-of-the-art PTM-based CIL approaches, while also exhibiting inherent robustness to data corruptions. Code is available at: <https://github.com/lemProg/PLASTIC>.

1 INTRODUCTION

In real-world applications, neural networks must continuously adapt to dynamic data streams that introduce new classes over time (Gomes et al., 2017). However, sequentially updating a model to accommodate new classes often leads to *catastrophic forgetting* (CF)—a phenomenon where newly acquired knowledge overwrites and erases previously learned information (French, 1999). To address this challenge, Class-Incremental Learning (CIL) has been introduced, enabling models to learn new classes continually from evolving data without losing the ability to classify previous classes using a unified classifier (Masana et al., 2022).

Traditional CIL methods often involve training networks from scratch on each new task (see Fig. 1 (a)), employing regularization techniques to mitigate CF (Masana et al., 2022; Wang et al., 2023a). However, the growing adoption of pre-trained models (PTMs) has transformed the CIL landscape, leveraging the strong generalization capabilities of PTMs to enhance learning efficiency. Many PTM-based CIL methods (Wang et al., 2022c;d;b; Villa et al., 2023; Smith et al., 2023) freeze the PTM backbone entirely and train only a small set of task-specific learnable parameters to condition the frozen representations. While these methods outperform traditional CIL approaches, they still require task-by-task fine-tuning, which remains computationally expensive, particularly in long task sequences.

To further reduce computational cost in CIL, recent works have shown that using a simple nearest class mean (NCM) (Mensink et al., 2013) classification with features extracted from PTMs can provide competitive results (Janison et al., 2022; Zhou et al., 2024a). This approach is further enhanced through *first session adaptation* (FSA) – often producing state-of-the-art results – consisting of fine-tuning the PTM *only* on the first task (Zhou et al., 2024a; Panos et al., 2023; McDonnell et al., 2024) while keeping it frozen for the rest to prevent CF. In essence, FSA aims at (i) *bridging the distribution gap* between the PTM pre-training and downstream tasks by training adapters (Chen et al., 2022b) on the first task, and (ii) *not risking forgetting* by confining fine-tuning only to the first task and keeping the PTM frozen thereafter. While FSA has proven effective, particularly for *homogeneous* task sequences—where all tasks share a similar data distribution (e.g., CIFAR-100 or ImageNet-A)—it assumes distributional uniformity across tasks. This assumption breaks down in *heterogeneous* settings, where tasks stem from diverse datasets (e.g., VTAB

datasets), resulting in substantial distribution shifts. Consequently, FSA methods, which rely on a frozen PTM after the first task, lack plasticity in such settings and struggle to adapt to evolving task distributions.

Given the inevitability of evolving task distributions, this work aims to *address the plasticity limitation of FSA approaches* when dealing with heterogeneous task distributions. To this end, we propose a novel approach that preserves the stability of FSA while introducing the necessary plasticity for adapting to diverse tasks. Our method, Plasticity-Enhanced Test-Time Adaptation in Class-Incremental Learning (PLASTIC), leverages Test-Time Adaptation (TTA) (Zhao et al., 2023; Sun et al., 2020; Zhang et al., 2021) to boost model plasticity using only unlabeled data from new tasks. TTA, which was originally designed for mitigating *domain shift* (Quinonero-Candela et al., 2008) between a pre-trained source model and the unlabelled data in the target domain (Liang et al., 2023).

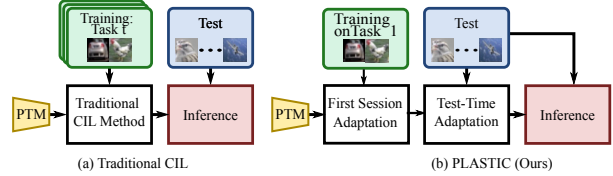


Figure 1: Comparison of traditional CIL methods with PLASTIC (Ours). (a) Traditional CIL methods entail training on each task’s training data, making it prone to forgetting. (b) In PLASTIC, we train the PTM only on the first task using Adapters, then adjust them for the subsequent tasks using Test-Time Adaptation and knowledge-distillation for better *stability-plasticity* trade-off.

TTA proves to be a natural fit for CIL by addressing its dual challenge: maintaining stability while ensuring adaptability to novel tasks. Specifically, PLASTIC leverages TTA to achieve: **(i) plasticity** by fine-tuning only a small subset of parameters of the PTM on the unlabelled test instance to adapt to any new task at hand; **(ii) stability** by employing a teacher-student distillation framework, where the teacher model guides adaptation and prevents the student from deviating excessively from the pre-trained representations, ensuring that task-specific updates remain stable while preserving generalization. However, naïve resetting after each TTA step discards past adaptations, preventing meaningful knowledge accumulation across tasks. To address this limitation, PLASTIC integrates student-teacher distillation, ensuring that adaptation remains continual rather than isolated to individual tasks. Specifically, the student model, initialized from the adapted PTM, undergoes TTA and is reset after each update. This design strikes a critical balance: on one hand, the student-teacher framework retains past learned representations, mitigating TTA’s limitation of discarding adaptation history. On the other hand, reinitializing the student from the PTM at each step preserves its pristine, generalizable representations, preventing harmful drift and ensuring robust adaptation across tasks. The framework is illustrated in Fig. 1 (b). Unlike Continual Test-Time Adaptation (CTTA) (Wang et al., 2022a; Song et al., 2023), which primarily addresses domain shifts by adapting models to evolving environmental conditions, PLASTIC is designed for CIL. We extend FSA by integrating TTA and incorporating model resetting mechanisms, thereby enabling the effective integration of new classes while maintaining model stability.

Unlike many CIL methods, PLASTIC is intuitive and simple to implement, yet delivers several benefits: **(i)** it reduces computation during training time by limiting the training to just the first task; **(ii)** Unlike FSA, PLASTIC allows greater adaptability to new tasks without excessive forgetting; **(iii)** By leveraging TTA, PLASTIC inherently withstands corruptions and perturbations (Hendrycks & Dietterich, 2019), a critical aspect often overlooked in CIL; and **(iv)** it is highly parameter-efficient. Through extensive experiments, we demonstrate that PLASTIC achieves state-of-the-art performance across standard CIL benchmarks, surpassing FSA methods. Moreover, by relying on TTA, PLASTIC is inherently robust to data corruptions, enhancing its real-world applicability.

2 RELATED WORK

Class-Incremental Learning is an active area of research (see the surveys in (Masana et al., 2022; Belouadah et al., 2021; Wang et al., 2023a; Parisi et al., 2019)) that deals with incrementally expanding the knowledge of a model to recognize new classes by training on labeled data arriving in sessions. While learning the new classes the model tends to forget previously acquired information due to the phenomenon called CF (French, 1999). Therefore, CIL methods aim at simultaneously balancing the knowledge acquisition (*i.e.*, *plasticity*) and retention (*i.e.*, *stability*) capabilities of the model (Mermillod et al., 2013). The CIL methods can be broadly categorized into four distinct groups. (i) Weight regularization CIL methods (Kirkpatrick et al., 2017; Liu et al., 2018; Zenke et al., 2017; Lee et al., 2020; Aljundi et al., 2018; Chaudhry et al., 2018) aim at preventing a drift in the weights of the network, which are relevant to the previous tasks. (ii) Data regularization CIL methods (Jung et al., 2016; Li & Hoiem, 2017; Rebuffi et al., 2017; Hou et al., 2019; Castro et al., 2018; Liu et al., 2020; Dhar et al., 2019; Douillard et al., 2020) instead aim at preventing drift in the network activation by employing knowledge distillation (Hinton et al., 2015). (iii) Memory rehearsal CIL methods reduce forgetting by storing and replaying a small number of exemplars (Rebuffi et al., 2017; Buzzega et al., 2020; Castro et al., 2018; Prabhu et al., 2020), or by generating synthetic images (Shin et al., 2017; Ostapenko et al.,

2019) or features (Xiang et al., 2019). (iv) Architecture growing CIL methods (Rusu et al., 2016; Mallya & Lazebnik, 2018; Mallya et al., 2018; Schwarz et al., 2018) dynamically increase the capacity of the network through allocating task-specific learnable parameters to prevent interference between tasks, and hence reduce forgetting. Our proposed PLASTIC is unique from most of the existing CIL literature as it operates directly at test-time. Although similar in spirit to GDumb (Prabhu et al., 2020), which re-trains the network at test-time from scratch using exemplars from the memory, our PLASTIC is *rehearsal-free* and requires only a single gradient update on the test sample.

CIL with Large Pre-Trained Models. With the introduction of large PTMs (Dosovitskiy et al., 2021a) the field of CIL has seen rapid progress (Wang et al., 2022d;c; Seale Smith et al., 2022; Zhou et al., 2024a; 2022; Zhang et al., 2023). It is mainly driven by the fact that PTMs are highly generalizable to downstream tasks and tuning only a small subset of parameters is sufficient to obtain good performance. Broadly speaking, all the PTM-based CIL methods can be classified under two categories. The *first category* consists of prompt-tuning (Jia et al., 2022) based CIL methods (Wang et al., 2022d;c; Seale Smith et al., 2022; Jung et al., 2023) that keep the PTM frozen and aim to train a set of learnable tokens (or prompts) on the training data to learn task-specific features. At inference, they query the prompt pool to retrieve a prompt pertaining to the test instance, and then condition the frozen PTM with the selected prompt. The prompt-tuning methods mostly differ in how the prompts are learned and how they are selected during inference. For instance, DualPrompt (Wang et al., 2022c) decomposes the prompts into general and expert prompts, whereas CODA-Prompt (Smith et al., 2023) refines the prompt selection using an attention mechanism. EASE (Zhou et al., 2024b) proposes to adaptively learn the projection subspace per task by injecting class-specific adapters in the PTM, to favor class separability-at the cost of more learnable parameters. The *second category* consists of conceptually simpler methods like ADAM (Zhou et al., 2024a) and FSA (Panos et al., 2023) that fine-tune adapters (Houlsby et al., 2019b) on the first task and keep the model unaltered for the remainder of tasks. RanPAC (McDonnell et al., 2024) extends this paradigm by training solely on the first task while applying random projections to subsequent tasks. CF is prevented by limiting the fine-tuning to only the first task at the cost of reduced plasticity. Differently from the existing methods, PLASTIC encourages plasticity via Test-Time Adaptation on every new task.

Test-Time Adaptation (TTA) has been proposed to improve the performance of a pre-trained model (trained on *source* data) on out-of-distribution test (or *target*) data, exhibiting domain-shift, by adjusting the model parameters using the unlabelled test samples (Liang et al., 2023; Wang et al., 2021; Sun et al., 2020; Liu et al., 2021; Zhang et al., 2021; Chen et al., 2022a; Bartler et al., 2022). In particular, the co-variate shift is simulated with synthetic corruptions (Hendrycks & Dietterich, 2019) (e.g., Gaussian noise, blur, shot noise) or natural shifts (e.g., sim to real (Peng et al., 2017)). The common theme among all TTA methods is to optimize an unsupervised loss (e.g., entropy minimization (Grandvalet & Bengio, 2004)) using the test instance and update either all the parameters of the network (Zhang et al., 2021) or only a subset (e.g., Batch Normalization layers (Wang et al., 2021)). Post adaptation, the resulting model is used for inference on the test instance, after which it is either reset back to the original checkpoint (Zhang et al., 2021) or directly used for the next adaptation steps (Wang et al., 2021). Different from the original motivation of TTA – to reduce domain shift between train and test data having overlapping classes – we exploit the generalizable PTM in CIL to adapt it to tasks (or datasets) containing a non-overlapping set of classes. Moreover, CIL differs from Continual Test-Time Adaptation (CTTA) methods such as CoTTA (Wang et al., 2022a; Song et al., 2023), (Machireddy et al., 2022), MetaMix (Wang et al., 2023c) and RMT (Döbler et al., 2023), which address domain shifts under a fixed label space. In contrast, CIL involves an evolving label space with each task. Additionally, while CTTA methods employ teacher-student frameworks with the teacher model as an exponential moving average (EMA) of the student, our approach utilizes the teacher to actively guide the student’s learning through a Kullback-Leibler (KL) divergence loss, enhancing adaptation in CIL scenarios. In contrast, we focus on adapting closed-vocabulary models (with Adapters (Chen et al., 2022b)) at TTA using entropy-minimization (Zhang et al., 2021) and further equip it with student-teacher distillation for exploiting past knowledge.

3 PROPOSED FRAMEWORK

3.1 PROBLEM FORMULATION AND OVERVIEW

CIL involves learning from a data stream that introduces new classes and aims to construct a unified classifier (Rebuffi et al., 2017). The training process consists of a sequence of T training tasks, denoted as $\mathcal{D} = \{\mathcal{D}^1, \mathcal{D}^2, \dots, \mathcal{D}^T\}$ with incremental data \mathcal{D}^t for each new task, each composed of K^t classes; hence, we have $K = \sum_{t=1}^T K^t$ total number of classes. For each class k , the number of training samples is N_k .

In this context, \mathbf{x}_i refers to a training instance belonging to the class $y_i \in Y^t$, where Y^t is the label space of task t . In our case, there is no overlap in the label spaces between different tasks, i.e., $Y^t \cap Y^{t'} = \emptyset$ for $t \neq t'$. During the t -th training stage, only data from \mathcal{D}^t can be accessed for model updates. Following the approach as in (Wang et al.,

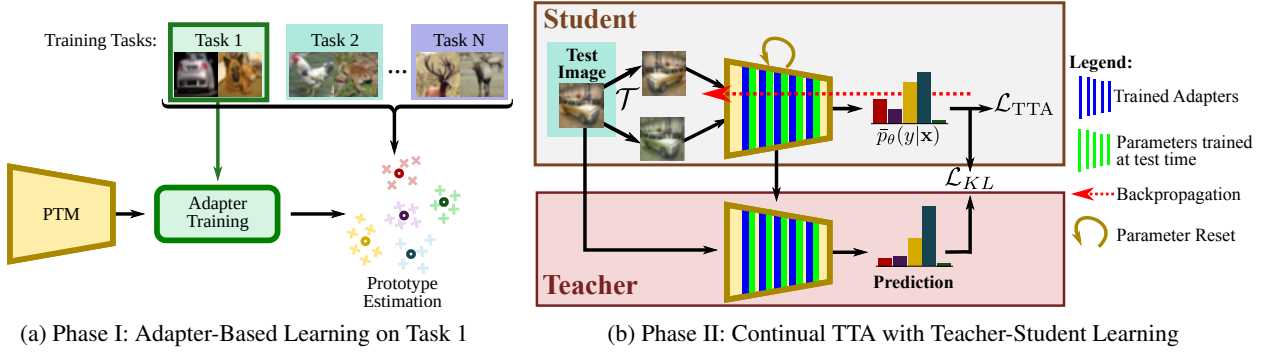


Figure 2: Our PLASTIC is composed of two phases. In **Phase I**, we fine-tune adapters on the first task’s training data in order to learn task-specific features. In **Phase II**, we perform TTA directly on the unlabelled test instances of each task. This allows the network to adapt to the intricate task-specific features from subsequent tasks, while not deviating too far from the generalizable PTM representations by using a teacher-student distillation framework, where the teacher model ensures stable learning.

2022d;c), we assume the availability of a PTM, such as a ViT (Dosovitskiy et al., 2021b) trained on the ImageNet-21K dataset (Ridnik et al., 2021). This PTM serves as the initialization for the CIL model. A successful CIL model f acquires knowledge from new classes while preserving it from the previously encountered ones. The evaluation of the model’s capability is performed across all seen classes, denoted as $\mathcal{Y}^T = Y^1 \cup \dots \cup Y^{t-1} \cup Y^t$, after each task t .

To address the challenge of balancing plasticity and stability in PTMs, we introduce PLASTIC, a novel method that employs a two-phase adaptation strategy. In Phase I, we adapt the PTM’s feature representations on the first task of the incremental setting (Sec. 3.2), as in FSA (Panos et al., 2023). Then, in Phase II we refine the model representations to counteract domain shifts and concept drift (Sec. 3.3) using a unique combination of TTA and knowledge distillation. This comprehensive approach, summarized in Fig. 2 and Algorithm 1, enables our model to maintain good stability, and enhanced plasticity for non-homogeneous tasks.

3.2 PHASE I: ADAPTING PTMS TO NEW TASKS

While NCM is a strong baseline in CIL (Janson et al., 2022), it offers no plasticity. The performance is unsatisfactory when downstream datasets exhibit domain shifts, especially with significant concept drift (Alfassy et al., 2022; Hendrycks et al., 2021b). To allow some plasticity, we employ an adaptation process, as in FSA methods (Zhou et al., 2024a; Panos et al., 2023), that bridges the distribution gap between the pre-training and the downstream task distribution. Fine-tuning is limited to the first task as repeated (or sequential) fine-tuning can trigger CF and weaken generalization (McDonnell et al., 2024; Kumar et al., 2022; Zhou et al., 2024a).

Formally, let E_θ be the PTM model’s feature extractor. We first compute class prototypes c_k for $k = 1$ by averaging the embeddings of each class in the first task (details in Supp. Mat.).

We adapt E_θ by inserting lightweight modules inside each layer called Adapters (Houlsby et al., 2019a). The adapter parameters, denoted as ϕ , are learned on the data \mathcal{D}^1 while the parameters θ of E_θ remain frozen. The adaptation is done by minimizing a Cross-Entropy loss using stochastic gradient descent. Importantly, the parameters ϕ represent a tiny proportion of the total number of parameters in $E_{\theta,\phi}$ (about 1% – 3%) to prevent over-fitting on \mathcal{D}^1 . This procedure provides an adapted feature extractor $E_{\theta,\phi}^*$ with domain-specific knowledge, while keeping the total number of trainable parameters minimal.

3.3 PHASE II: CONTINUAL TEST-TIME MODEL REFINEMENT

At the end of Phase I, the adapted PTM is adept at classifying samples from the first task and exhibits strong performance on the subsequent tasks with the NCM classifier under the assumption that task distributions remain unaltered. Given that this assumption is vacuous when subsequent tasks are heterogeneous in nature, we propose to improve the plasticity with continual test-time model refinement by directly using the unlabelled test instances. This phase consists of test-time refinement and teacher-student distillation, which are explained below.

Test-time refinement. After the initial adaptation on the first task, our model may still provide unsatisfactory results when it encounters visual content different from the past tasks (see Fig. 3). To tackle this, we propose to employ

Test-Time Adaptation (TTA), which enables plasticity without suffering from CF. This TTA phase consists of a slight feature adaptation on the test images in an unsupervised fashion. After evaluation on each test batch, our model is reset to the initial state $E_{\theta, \phi}^*$ to maintain generalizability, and we prevent CF (Fleuret et al., 2021; Zhang et al., 2021). An additional reason for adopting a TTA approach is that it enhances the robustness of our model against noisy and corrupted samples during inference (Sun et al., 2020; Wang et al., 2021). Inspired by MEMO (Zhang et al., 2021), given a test sample \mathbf{x}_i , an adapted PTM model (from Phase I), and a set of image transformations \mathcal{T} , we pick M random transformations $\{\tau_1, \dots, \tau_M\}$ from \mathcal{T} and apply them to \mathbf{x}_i to produce a batch of augmented data $\{\tilde{\mathbf{x}}_{i,1}, \dots, \tilde{\mathbf{x}}_{i,M}\}$. The marginal output distribution for the augmented points is given by:

$$\bar{p}_{\theta, \phi}(y|\mathbf{x}_i) \approx \frac{1}{M} \sum_{m=1}^M p_{\theta, \phi}(y|\tilde{\mathbf{x}}_{i,m}). \quad (1)$$

We propose to adapt the model by minimizing the entropy of its marginal output distribution over augmentations equation 1:

$$\mathcal{L}_{\text{TTA}}(\theta, \phi; \mathbf{x}_i) = - \sum_{y \in \mathcal{Y}} \bar{p}_{\theta, \phi}(y|\mathbf{x}_i) \log \bar{p}_{\theta, \phi}(y|\mathbf{x}_i). \quad (2)$$

Minimizing equation 2 encourages both high confidence and invariance to input augmentations.

Specifically, the entropy term $\bar{p}_{\theta, \phi}(\cdot|\mathbf{x}_i)$ reaches its minimum value when the model delivers consistent and confident predictions, regardless of the particular data augmentation applied. The motivation for optimizing the model to yield more confident predictions is grounded in the belief that the decision boundaries distinguishing classes are situated in areas of the data space with lower density (Grandvalet & Bengio, 2004; Zhang et al., 2021). As $\bar{p}_{\theta, \phi}(y|\mathbf{x}_i)$ is differentiable with respect to θ based on the loss defined in equation 2, we can employ gradient-based optimization directly to adapt θ . Test-time adaptation requires careful selection of parameters (Niu et al., 2022), our adaptation procedure focuses solely on adapting the *layer-norm* parameters (Ba et al., 2016), unlike MEMO (Zhang et al., 2021), which finetunes the entire model. We found that adapting all the parameters hurts the performance (see Sec. 4.3). Only one gradient step per test point is empirically determined to be sufficient for achieving improved performance, with less inference time overhead.

While TTA is a simple and effective solution for CIL, it does not fully conform to the tenets of continual learning as TTA involves model reset after each batch update (Zhang et al., 2021), erasing all past updates. Moreover, although TTA can also be realized *without* resetting its weights, such an approach will be prone to CF and reduced PTM generalization. To fully capitalize the past updates and prevent overfitting on the current batch (see Sec. 4.3), a regularization strategy is proposed, which is discussed next.

Teacher-student distillation. We propose to distill the past (and potentially useful) knowledge while performing TTA on a current test batch through a teacher-student distillation strategy. Formally, the teacher model E_{θ_T, ϕ_T} is initially a copy of the student model before adaptation begins. Throughout the TTA phase, the student model is updated with each test batch as explained above. After each batch, the teacher model’s predictions are used to provide soft targets for the student model. These predictions are compared to the student model’s outputs using Kullback-Leibler (KL) divergence (Kullback & Leibler, 1951). For simplification, we omit the parameters of Adapters ϕ from the equations, since they are frozen during Phase II. Thus, the KL-divergence loss is defined as follows:

$$\mathcal{L}_{KL}(\theta_T, \theta_S) = \sum_{y \in \mathcal{Y}} p_{\theta_S}(y | \tilde{\mathbf{x}}_i) \log \frac{p_{\theta_S}(y | \tilde{\mathbf{x}}_i)}{p_{\theta_T}(y | \tilde{\mathbf{x}}_i)}, \quad (3)$$

where $p_{\theta_T}(y | \tilde{\mathbf{x}}_i)$ and $p_{\theta_S}(y | \tilde{\mathbf{x}}_i)$ represent the teacher and student model’s probability distributions over the class labels y , respectively, for the augmented input $\tilde{\mathbf{x}}_i$.

Overall, this teacher-student distillation approach helps in transferring the improved feature representation and decision boundaries learned by the teacher model to the student model, thereby benefiting from the TTA phase and

Algorithm 1 PLASTIC.

Require: Sequence of T tasks, $\mathcal{D} = \mathcal{D}^1, \dots, \mathcal{D}^T$, and pre-trained model f

- 1: **Phase I:** *Adapting PTMs to New Tasks*
- 2: Adapt model f using Adapters on \mathcal{D}^1 .
- 3: **Phase II:** *Test-Time Model Refinement*
- 4: **Initiate** student/teacher models.
- 5: **for** a batch \mathcal{X} in \mathcal{D}_{test}^t **do**
- 6: **for** iteration $n = 1 \dots N$ **do**
- 7: Sample transformations from \mathcal{T} and apply to \mathcal{X} .
- 8: Calculate predictions via equation 1.
- 9: Adapt parameters via equation 4.
- 10: **end for**
- 11: **Update** the teacher model via equation 5.
- 12: **Reset** the student model.
- 13: **end for**
- 14: **return** predictions for all $\mathbf{x}_i \in \mathcal{D}_{test}^t$.

Table 1: Average ($\bar{\mathcal{A}}$) and last performance (\mathcal{A}_T) comparison on six datasets with **ViT-B/16-IN21K** backbone. “IN-R/A” stands for “ImageNet-R/A”, and “OmniBench” stands for “OmniBenchmark”. LwF, L2P, DualPrompt, and Coda-Prompt results are from (Zhou et al., 2024a). The best performance is in bold, and the second best is underlined.

	Method	CIFAR100-Inc5		CUB-Inc10		IN-R-Inc5		IN-A-Inc10		OmniBench-Inc30		VTAB-Inc10		Average $\bar{\mathcal{A}}$
		$\bar{\mathcal{A}}$	\mathcal{A}_T	$\bar{\mathcal{A}}$	\mathcal{A}_T	$\bar{\mathcal{A}}$	\mathcal{A}_T	$\bar{\mathcal{A}}$	\mathcal{A}_T	$\bar{\mathcal{A}}$	\mathcal{A}_T	$\bar{\mathcal{A}}$	\mathcal{A}_T	
	NCM	86.27	81.27	90.79	86.77	61.63	54.33	58.66	48.52	80.63	73.33	85.99	84.44	77.33
Sequential Updating	Finetune	38.90	20.17	26.08	13.96	21.61	10.79	21.60	10.96	23.61	10.57	34.95	21.25	27.79
	Finetune Adapter (Chen et al., 2022b)	60.51	49.32	66.84	52.99	47.59	40.28	43.05	37.66	62.32	50.53	48.91	45.12	54.87
	LwF (Li & Hoiem, 2017)	46.29	41.07	48.97	32.03	39.93	26.47	35.39	23.83	47.14	33.95	40.48	27.54	43.03
	L2P (Wang et al., 2022d)	85.94	79.93	67.05	56.25	66.53	59.22	47.16	38.48	73.36	64.69	77.11	77.10	69.53
	DualPrompt (Wang et al., 2022c)	87.87	81.15	77.47	66.54	63.31	55.22	52.56	42.68	73.92	65.52	83.36	81.23	73.08
	Coda-Prompt (Smith et al., 2023)	89.11	81.96	84.00	73.37	64.42	55.08	53.54	42.73	77.03	68.09	83.90	83.02	75.33
	SLCA (Zhang et al., 2023)	94.54	91.19	84.70	81.76	74.10	69.73	61.98	56.48	80.40	72.05	88.92	82.65	80.77
First Session Adaptation	EASE (Zhou et al., 2024b)	91.51	85.80	<u>91.01</u>	<u>86.81</u>	78.01	70.58	<u>65.80</u>	<u>56.87</u>	<u>81.03</u>	<u>74.85</u>	92.61	90.55	<u>83.32</u>
	FSA-FiLM (Panos et al., 2023)	90.13	86.23	91.23	86.12	73.65	65.13	60.11	49.53	80.64	74.09	87.47	82.12	80.53
	ADAM (Zhou et al., 2024a)	90.87	85.15	91.06	86.73	72.35	64.33	60.21	49.57	79.70	55.24	85.95	84.35	80.02
	RanPAC (McDonnell et al., 2024)	<u>93.14</u>	<u>89.05</u>	<u>91.56</u>	85.91	77.60	68.03	61.84	46.02	80.27	74.46	<u>91.75</u>	<u>90.32</u>	82.69
	FeCAM (Goswami et al., 2023)	88.97	85.34	92.16	88.59	70.13	65.17	56.78	47.27	83.34	73.03	94.14	89.12	80.92
	PLASTIC (w/o Phase I)	85.71	82.54	89.55	85.75	61.96	55.13	60.46	50.43	81.05	73.84	89.93	85.17	78.11
	PLASTIC	92.34	88.58	91.24	86.95	<u>76.88</u>	<u>69.93</u>	67.04	57.41	81.13	76.39	91.57	86.38	83.36

Table 2: Average performance ($\bar{\mathcal{A}}$) comparison with **ViT-B/16-IN21K** as the backbone on three corrupted benchmarks CIFAR100-C, VTAB-C and OmniBench-C with Level-5 noise corruptions (Hendrycks & Dietterich, 2019). The best performance is in bold, and the second best is underlined.

Method	CIFAR100-C				VTAB-C				OmniBench-C			
	Gauss.	Shot	Impul.	Avg.	Gauss.	Shot	Impul.	Avg.	Gauss.	Shot	Impul.	Avg.
NCM	35.52	39.05	46.89	40.48	69.64	72.31	58.18	66.71	77.44	78.43	75.07	76.98
ADAM (Zhou et al., 2024a)	37.52	48.73	65.03	<u>50.43</u>	71.10	74.11	58.98	<u>68.06</u>	79.45	79.57	77.76	<u>78.93</u>
PLASTIC	48.87	53.38	68.61	56.95	71.58	74.23	59.44	68.41	79.70	79.81	78.41	79.31

enhancing the robustness of the final model. The overall loss during Phase II is given by:

$$\mathcal{L}_{\text{total}}(\theta_S, \theta_T; \mathbf{x}_i) = \mathcal{L}_{\text{TTA}}(\theta_S; \mathbf{x}_i) + \lambda \mathcal{L}_{\text{KL}}(\theta_T, \theta_S), \quad (4)$$

where λ is a hyperparameter that controls the weight of the KL-divergence loss relative to the TTA loss.

To ensure that the teacher model effectively incorporates the student’s learned information, we update the teacher using an Exponential Moving Average (EMA) of the student’s parameters after each test batch. EMA helps in transferring the learned representations, which would otherwise be lost in TTA. The EMA update is given by:

$$\theta_T = \alpha \theta_T + (1 - \alpha) \theta_S, \quad (5)$$

where θ_T and θ_S denote the teacher and student parameters, respectively, and α is the smoothing factor (with $0 < \alpha < 1$). Afterward, the student model is reset after each batch to incorporate effective adaptation on the test samples and avoid degradation of performance (see Sec. 4.3).

4 EXPERIMENTS

4.1 EXPERIMENTAL SETUP

Datasets and settings. We validate PLASTIC on seven CIL benchmarks. In detail, following the work in (Zhou et al., 2024a) we experiment with CIFAR100 (Krizhevsky et al., 2009), CUB200 (Wah et al., 2011), ImageNet-R (Hendrycks et al., 2021a), ImageNet-A (Hendrycks et al., 2021b), OmniBench (Zhang et al., 2022), 5-Datasets (Wang et al., 2022d) and VTAB (Zhou et al., 2024a). All these benchmarks offer diverse levels of difficulty in terms of high task heterogeneity (e.g. 5-Datasets, VTAB) or large domain gap to ImageNet (e.g. ImageNet-A). For the experiments on robustness, we pick three benchmarks: CIFAR100-C (Hendrycks & Dietterich, 2019), OmniBench-C, and VTAB-C, where “C” stands for corrupted counterparts of the original benchmarks. In this work, we introduce the VTAB-C and OmniBench-C by adding the same corruptions as in CIFAR100-C to the original testing sets of VTAB and OmniBench benchmarks, respectively.

We follow the incremental settings established in (Zhou et al., 2024a), i.e. by adopting an increment per task of three types: 5 classes (Inc5) for CIFAR100 and ImageNet-R; 10 classes (Inc10) for CUB200, ImageNet-A, VTAB, and 5-Datasets; and 30 classes (Inc30) for OmniBench. The same increments and task orders are followed in the robustness experiments. Finally, we evaluate all the methods in *task-agnostic* manner, i.e., without having access to the task-id at inference. More details are available in the Supp. Mat.

Implementation details. Following ADAM (Zhou et al., 2024a), we have used ViT-B/16 (Dosovitskiy et al., 2021b) initially pre-trained on ImageNet-21K and further fine-tuned on ImageNet-1K, as a backbone. For Phase I, we trained the adapters (one adapter per ViT block) using Stochastic Gradient Descent (SGD) with momentum for 20 epochs, with an initial learning rate of 0.01 that undergoes cosine annealing. In Phase II we have used a batch size of 16 and augmented each test sample 8 times using random image transformations (Zhang et al., 2021). As mentioned before, for one mini-batch, we do one gradient step in Phase II to obtain the adapted model. The learning rate is set to 0.01, no weight decay is employed, $\lambda=0.1$, and $\alpha=0.99$. We use PILOT (Sun et al., 2023) framework for our experiments.

Baselines and competitors. We have compared PLASTIC with state-of-the-art PTM-based CIL methods: LwF (Kirkpatrick et al., 2017), L2P (Wang et al., 2022d), DualPrompt (Wang et al., 2022c), ADAM (Zhou et al., 2024a), FSA-FiLM (Panos et al., 2023), EASE (Zhou et al., 2024b), FeCAM (Goswami et al., 2023) and SLCA (Zhang et al., 2023). All methods are initialized with the same PTM (ViT-B-16 (Dosovitskiy et al., 2021b)) pre-trained on Imagenet-21K. Additionally, we have compared with two more baselines: Finetune and Finetune Adapter (Chen et al., 2022b).

Evaluation Metrics. In alignment with (Zhou et al., 2024a;b), we employ two key performance indicators: (i) \mathcal{A}_T , representing the Top-1 accuracy after learning the final task, and (ii) $\bar{\mathcal{A}}$, calculated as the average Top-1 accuracy while learning progresses in incremental steps. Additionally, we report the standard deviation for both metrics computed over five independent trials (seeds).

4.2 MAIN RESULTS

Results on standard CIL benchmarks. We report in Tab. 1 the empirical evaluation on the standard CIL benchmarks. The results show that PLASTIC achieves the best performance, with an average accuracy $\bar{\mathcal{A}}$ of 83.36%, the highest among all methods. Notably, PLASTIC consistently outperforms ADAM (Zhou et al., 2024a) and RanPAC (McDonnell et al., 2024) on most benchmarks, including challenging datasets like ImageNet-A and OmniBench. While SLCA and EASE slightly outperform PLASTIC on specific datasets like CIFAR100 and VTAB, their competitive results stem from their ability to train significantly more parameters—SLCA fine-tunes all model parameters, and EASE introduces a new adapter for each task. This increased plasticity comes at the cost of substantial computational overhead, making these methods less efficient and scalable compared to PLASTIC. Compared to ADAM, PLASTIC shows a substantial improvement, with a gap of +3.34% in average performance (83.36% vs 80.02%). If adapters are fine-tuned on each task, as seen in the Finetune Adapter baseline, the final performance drops drastically to 54.87%, highlighting the severe downsides of task-specific fine-tuning. PLASTIC w/o Phase I achieves competitive results with an average accuracy of 78.11%, which is still a notable improvement over the baseline NCM (+0.78%).

Results on CIL benchmarks with corruptions. In Tab. 2 we report the empirical evaluation on CIL benchmarks with different kinds of noise corruptions (of level 5 (Hendrycks & Dietterich, 2019)), where we compare our proposed PLASTIC with the competitors. In ADAM and our PLASTIC, *we exclude training on the clean samples from every task, except the first task*. The NCM exhibits the worst performance as it solely relies on the representation learned from the pre-training dataset. ADAM, which trains the network on the training data from the first task, shows an improvement in performance due to better adaptivity to the NCM. PLASTIC achieves the best performance as it further allows the model to adapt towards every subsequent task. In particular, the gain in performance is significant for CIFAR100-C, where our proposed PLASTIC outperforms ADAM by +5.33%.

In summary, PLASTIC satisfies three desiderata: (i) improved adaptivity to new tasks; (ii) less computational cost by avoiding sequential training on each task; and (iii) robustness to corruptions by refining its predictions on the corrupted test instances during test-time. We report the results on other types of corruption in the Supp. Mat.

4.3 ABLATION STUDY

① **Effect of task ordering.** In Fig. 3 we study the influence of task order, especially in the case of heterogeneous tasks. We choose to perform experiments on the 5-Datasets benchmark (Wang et al., 2022c) as it contains five very heterogeneous datasets: SVHN, MNIST, CIFAR10, NotMNIST, and FashionMNIST. Here we mainly compare PLASTIC with ADAM as both undergo training on the first task’s data. From Fig. 3, we notice that a different task order yields different performance for PLASTIC and ADAM, indicating that the first task plays an important role in determining the final performance. However, in all the task orderings, PLASTIC outperforms ADAM by big margins, with the highest margin (+10.29%) obtained in the tasks of order SVHN → MNIST → CIFAR10 → NotMNIST → FashionMNIST. This highlights that the data from the second task onwards, despite *unlabelled*, offer a learning signal that is efficiently exploited by our PLASTIC during Phase II. Differently, as ADAM does not offer any plasticity after the first task, it fails to improve the adaptivity on future tasks.

We can also observe that when the first task is CIFAR10, a dataset very different from the other tasks, PLASTIC still yields a performance gain over both ADAM and NCM. These results are promising since they indicate that PLASTIC is a relevant solution even when the domain shifts in future tasks are potentially large (Prabhu et al., 2023).

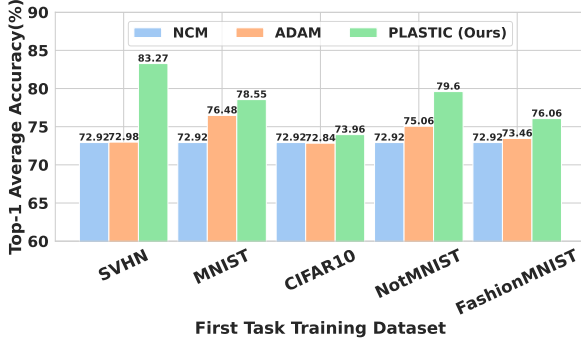


Figure 3: Impact of initial task on model performance. X-axis: first training task. Y-axis: average performance across datasets for NCM, ADAM, and PLASTIC. Performance varies with task order, highlighting the importance of the initial task.

② **Effect of the adaptation parameters.** The experiments presented in Tab. 3 focus on evaluating different parameters to adapt, and the effect of model resetting during *Test-Time Model Refinement phase*. We compare: (i) *no TTA* – we do not apply test-time adaptation (equivalent to ADAM (Zhou et al., 2024a)); (ii) *All* – we adapt all the parameters of the model; (iii) *Adapter* – we adapt only the parameters of the adapter; and (iv) *Norm* – we adapt only the Layer Norm.

Adapting all the parameters results in 87M trainable parameters, yielding lower VTAB and Imagenet-R accuracies of 43.26% and 26.02% respectively, likely due to the inherent complexity of adapting with few samples, and to one optimization iteration. The adapter-only update reduces trainable parameters to 1.2M, improving VTAB and Imagenet-R accuracies to 89.89% and 75.28%. The most efficient performance is achieved by updating only 0.04M Layer Norm parameters, aligning with Niu et al.’s (Niu et al., 2023) findings on norm-layer adaptations enhancing stability in TTA. Further, our approach achieves superior efficiency by requiring significantly fewer trainable parameters while maintaining high performance. We provide a computational complexity analysis and a comparison of trainable parameters against other baselines in the supplementary material, highlighting this advantage.

③ **Effect of Student-Teacher distillation.** Tab. 4 presents a study analyzing the contribution of two core components in the PLASTIC: the *student reset* and the *KL divergence loss* (equation 3) used for distillation between student and teacher. Without student resetting, performance drops significantly—down to 43.31% on VTAB and 41.77% on ImageNet-A—due to cumulative overfitting and knowledge degradation (Zhao et al., 2023).

Resetting the student to the adapted pre-trained model mitigates this drift by reinitializing adaptation from a model with strong generalization ability, thereby reducing variance and overfitting. However, resetting alone is not sufficient, as the student—despite being reinitialized—can still overfit to the current batch during adaptation. To mitigate this, we incorporate a KL divergence loss from the teacher to the student. This loss acts as a regularization signal, guiding the student to adapt while remaining close to the teacher’s stable representation, which encapsulates previously accumulated knowledge. In parallel, the teacher model is updated via an EMA of the student, allowing it to gradually integrate useful information across batches without being overly influenced by any single adaptation step. Together, the KL loss and reset mechanism ensure that adaptation is stable and knowledge accumulation.

④ **Effect of TTA.** Our analysis proposed in Tab. 5 focuses on the effectiveness of different TTA methods—specifically TENT (Wang et al., 2021), MEMO (Zhang et al., 2021), and SAR (Niu et al., 2023)—in PLASTIC while constraining fine-tuning to layer-norm (Ba et al., 2016).

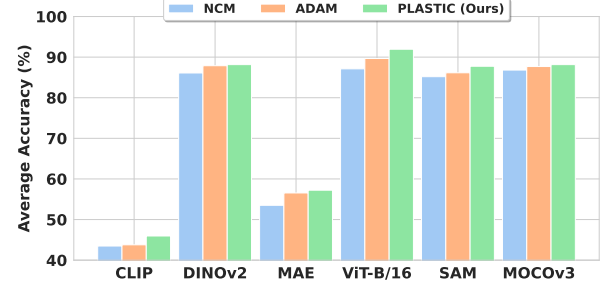


Figure 4: Evaluation with different PTMs on VTAB. PLASTIC consistently improves the performance of ADAM and NCM.

Table 3: Performance of PLASTIC with various optimized parameters during Phase II. M: Trainable parameters in millions (\downarrow).

		# Par. (M) \downarrow	VTAB (\bar{A}) \uparrow	ImageNet-R (\bar{A}) \uparrow
TTA	No TTA	0	85.68 \pm 2.44	72.35 \pm 1.11
	All	87	43.26 \pm 1.15	26.02 \pm 0.39
	Adapter	1.2	89.89 \pm 0.64	75.28 \pm 0.97
	Norm	0.04	91.57 \pm 0.64	76.88 \pm 0.42

Table 4: Impact of distillation framework components.

Reset	\mathcal{L}_{KL}	VTAB (\bar{A}) \uparrow	ImageNet-A (\bar{A}) \uparrow
		43.31 \pm 7.34	41.77 \pm 9.29
	✓	59.15 \pm 3.85	43.12 \pm 4.08
✓	✓	91.57 \pm 0.64	67.04 \pm 0.53

Table 5: Evaluation of TTA methods in PLASTIC.

Method	VTAB (\bar{A}) \uparrow	ImageNet-A (\bar{A}) \uparrow
TENT (Wang et al., 2021)	81.21 \pm 0.87	61.40 \pm 0.70
SAR (Niu et al., 2023)	83.79 \pm 1.15	55.69 \pm 1.92
MEMO (Zhang et al., 2021)	91.57 \pm 0.64	67.04 \pm 0.53

The evaluation of TTA methods in PLASTIC reveals distinct performance trends: MEMO consistently outperforms TENT and SAR, achieving the highest VTAB (91.28%) and ImageNet-A (67.04%) accuracies with minimal variance. SAR surpasses TENT on VTAB but exhibits higher variability. These results suggest that TENT and SAR’s effectiveness depends on dataset characteristics and task requirements (Zhao et al., 2023).

⑤ Effect of the test samples order. We assess PLASTIC’s sensitivity to test sample order, a critical factor in real-world applications. Tab. 6 reports results from five random seeds on VTAB, ImageNet-R, and ImageNet-A. PLASTIC demonstrates strong robustness, maintaining consistently high performance with low variance across datasets. Notably, VTAB results show exceptional stability (90.60 ± 1.87 in $\bar{\mathcal{A}}$, 86.02 ± 0.31 in \mathcal{A}_T).

Table 6: Robustness of PLASTIC to test sample order across datasets.

Method	$\bar{\mathcal{A}} \uparrow$	$\mathcal{A}_T \uparrow$
VTAB	90.60 ± 1.87	86.02 ± 0.31
ImageNet-A	66.46 ± 1.37	55.72 ± 1.29
ImageNet-R	76.62 ± 0.59	70.66 ± 0.13

The consistency across seeds indicates that PLASTIC effectively learns from the test distribution without overfitting to specific batch orders. We attribute this robustness to our adapted student-teacher distillation framework, which facilitates continuous learning while mitigating overfitting to temporary distribution shifts.

⑥ Effect of the PTM backbone. Here we evaluate, on VTAB, the influence of pre-trained models (PTMs). The analysis in in Fig. 4 incorporates PTMs such as ViT-B/16-IN1K/21K, ViT-B/16-DINO (Caron et al., 2021), ViT-B/16-SAM (Chen et al., 2022c), ViT-B/16-MAE (He et al., 2022), and ViT-B/16-CLIP (Radford et al., 2021) (image encoder). ViTs trained with supervised loss demonstrate enhanced performance over unsupervised counterparts. CLIP’s performance on the VTAB benchmark is the lowest, as indicated by Radford et al. (Radford et al., 2021). CLIP features for VTAB dataset subsets show reduced discriminability, leading to lower performance compared to alternative backbones. Furthermore, the nature of the pre-training task contributes to MAE’s modest results on the VTAB benchmark. In summary, PLASTIC surpasses ADAM across all backbones, attributed to the improvement during TTA.

⑦ Effect of the hyperparameters. We investigate the influence of iterative adjustments during the *test-time model refinement* phase. The results are summarized in Tab. 7. Increasing the number of test-time iterations resulted in a decrease in performance on both datasets, due to overfitting on low-entropy samples, thereby impairing the model’s generalization (Niu et al., 2022; Zhao et al., 2023). Overfitting to low-entropy samples leads to inaccuracies in classifying more complex or higher-entropy samples within the same batch, highlighting a trade-off

Table 7: Effect of adaptation iterations N .

Iterations	VTAB ($\bar{\mathcal{A}}$) \uparrow	Imagenet-R ($\bar{\mathcal{A}}$) \uparrow
$N = 1$	91.28 ± 0.64	76.88 ± 1.02
$N = 2$	<u>87.34</u> ± 3.05	<u>74.77</u> ± 1.22
$N = 3$	84.07 ± 3.53	70.14 ± 3.35
$N = 4$	80.78 ± 5.45	69.13 ± 2.08

between adaptability and overfitting. We also investigated the influence of batch size, number of adaptation iterations, and augmentations per iteration on model performance (see Supp. Mat.).

4.4 DISCUSSION

① Computational complexity. The main limitations of PLASTIC are its computational complexity and its high inference time. Phase II requires extra computation before each prediction, but this increased computation cost is a trade-off for improved plasticity and robustness. Practically, PLASTIC can still perform inference at 8 frames per second when using a single TTA iteration (see Supp. Mat.). Furthermore, this increase in inference time is balanced by PLASTIC’s computational efficiency during training, *i.e.*, by updating only the Adapter parameters in the first task.

② Practical benefits. The additional test-time overhead of PLASTIC is also balanced by the greater computational efficiency in the training phase, necessitating parameter updates solely on the first task. This contrasts with conventional CIL strategies, which require fine-tuning of PTMs across all tasks (Zhang et al., 2023). Therefore, PLASTIC leads to a reduction in communication costs for the CIL model to multiple clients in a distributed inference system (Mofrad et al., 2020; Mohammed et al., 2020).

5 CONCLUSIONS AND FUTURE WORK

We introduced PLASTIC, a novel approach to CIL that integrates the stability of First Session Adaptation with the plasticity of Test-Time Adaptation. PLASTIC effectively adapts to both homogeneous and heterogeneous task distributions while preserving the generalization capabilities of pre-trained models. Our method achieves state-of-the-art performance on standard CIL benchmarks, demonstrating enhanced plasticity and inherent robustness to data corruptions. Future research will focus on further improving PLASTIC’s efficiency and scalability, particularly by leveraging advanced sampling strategies (Niu et al., 2022; Wang et al., 2023b) to improve inference time.

Acknowledgements. This paper has been supported by the French National Research Agency (ANR) in the framework of its JCJC, and was funded by the European Union’s Horizon Europe research and innovation program under grant agreement No. 101120237 (ELIAS). Furthermore, this research was partially funded by Hi!PARIS Center on Data Analytics and Artificial Intelligence. This work was also supported in part by project SERICS (PE00000014) under the NRRP MUR program funded by the EU - NGEU. This work was granted access to the HPC resources of IDRIS under the allocation AD011013860 made by GENCI.

REFERENCES

- Amit Alfassy, Assaf Arbelle, Oshri Halimi, Sivan Harary, Roei Herzig, Eli Schwartz, Rameswar Panda, Michele Dolfi, Christoph Auer, Peter Staar, et al. Feta: Towards specializing foundational models for expert task applications. *Adv. Neural Inform. Process. Syst.*, 2022.
- Rahaf Aljundi, Francesca Babiloni, Mohamed Elhoseiny, Marcus Rohrbach, and Tinne Tuytelaars. Memory aware synapses: Learning what (not) to forget. In *Eur. Conf. Comput. Vis.*, 2018.
- Jimmy Lei Ba, Jamie Ryan Kiros, and Geoffrey E. Hinton. Layer normalization, 2016.
- Alexander Bartler, Andre Bühler, Felix Wiewel, Mario Döbler, and Bin Yang. Mt3: Meta test-time training for self-supervised test-time adaption. In *ICAIC*. PMLR, 2022.
- Eden Belouadah, Adrian Popescu, and Ioannis Kanellos. A comprehensive study of class incremental learning algorithms for visual tasks. *Neural Networks*, 135, 2021.
- Pietro Buzzega, Matteo Boschini, Angelo Porrello, Davide Abati, and Simone Calderara. Dark experience for general continual learning: a strong, simple baseline. *Adv. Neural Inform. Process. Syst.*, 33, 2020.
- Mathilde Caron, Hugo Touvron, Ishan Misra, Hervé Jégou, Julien Mairal, Piotr Bojanowski, and Armand Joulin. Emerging properties in self-supervised vision transformers. In *Int. Conf. Comput. Vis.*, 2021.
- Francisco M Castro, Manuel J Marín-Jiménez, Nicolás Guil, Cordelia Schmid, and Karteek Alahari. End-to-end incremental learning. In *Eur. Conf. Comput. Vis.*, 2018.
- Arslan Chaudhry, Puneet K Dokania, Thalaiyasingam Ajanthan, and Philip HS Torr. Riemannian walk for incremental learning: Understanding forgetting and intransigence. In *Eur. Conf. Comput. Vis.*, 2018.
- Dian Chen, Dequan Wang, Trevor Darrell, and Sayna Ebrahimi. Contrastive test-time adaptation. In *IEEE Conf. Comput. Vis. Pattern Recog.*, 2022a.
- Shoufa Chen, GE Chongjian, Zhan Tong, Jiangliu Wang, Yibing Song, Jue Wang, and Ping Luo. Adaptformer: Adapting vision transformers for scalable visual recognition. In *Adv. Neural Inform. Process. Syst.*, 2022b.
- Xiangning Chen, Cho-Jui Hsieh, and Boqing Gong. When vision transformers outperform resnets without pre-training or strong data augmentations. In *Int. Conf. Learn. Represent.*, 2022c.
- Prithviraj Dhar, Rajat Vikram Singh, Kuan-Chuan Peng, Ziyang Wu, and Rama Chellappa. Learning without memorizing. In *IEEE Conf. Comput. Vis. Pattern Recog.*, 2019.
- Mario Döbler, Robert A Marsden, and Bin Yang. Robust mean teacher for continual and gradual test-time adaptation. In *Proceedings of the IEEE/CVF Conference on Computer Vision and Pattern Recognition*, pp. 7704–7714, 2023.
- Alexey Dosovitskiy, Lucas Beyer, Alexander Kolesnikov, Dirk Weissenborn, Xiaohua Zhai, Thomas Unterthiner, Mostafa Dehghani, Matthias Minderer, Georg Heigold, Sylvain Gelly, Jakob Uszkoreit, and Neil Houlsby. An image is worth 16x16 words: Transformers for image recognition at scale. In *Int. Conf. Learn. Represent.*, 2021a.
- Alexey Dosovitskiy, Lucas Beyer, Alexander Kolesnikov, Dirk Weissenborn, Xiaohua Zhai, Thomas Unterthiner, Mostafa Dehghani, Matthias Minderer, Georg Heigold, Sylvain Gelly, Jakob Uszkoreit, and Neil Houlsby. An image is worth 16x16 words: Transformers for image recognition at scale. In *Int. Conf. Learn. Represent.*, 2021b.
- Arthur Douillard, Matthieu Cord, Charles Ollion, Thomas Robert, and Eduardo Valle. Podnet: Pooled outputs distillation for small-tasks incremental learning. In *Eur. Conf. Comput. Vis.*, 2020.
- Sayna Ebrahimi, Franziska Meier, Roberto Calandra, Trevor Darrell, and Marcus Rohrbach. Adversarial continual learning. In *Eur. Conf. Comput. Vis.*, 2020.

- François Fleuret et al. Test time adaptation through perturbation robustness. In *Adv. Neural Inform. Process. Syst. Worksh.*, 2021.
- Robert M French. Catastrophic forgetting in connectionist networks. *Trends in cognitive sciences*, 3(4), 1999.
- Heitor Murilo Gomes, Jean Paul Barddal, Fabrício Enembreck, and Albert Bifet. A survey on ensemble learning for data stream classification. *CSUR*, 50(2), 2017.
- Dipam Goswami, Yuyang Liu, Bartłomiej Twardowski, and Joost Van De Weijer. Fecam: Exploiting the heterogeneity of class distributions in exemplar-free continual learning. *Advances in Neural Information Processing Systems*, 36: 6582–6595, 2023.
- Yves Grandvalet and Yoshua Bengio. Semi-supervised learning by entropy minimization. *Adv. Neural Inform. Process. Syst.*, 17, 2004.
- Kaiming He, Xinlei Chen, Saining Xie, Yanghao Li, Piotr Dollár, and Ross Girshick. Masked autoencoders are scalable vision learners. In *IEEE Conf. Comput. Vis. Pattern Recog.*, 2022.
- Dan Hendrycks and Thomas Dietterich. Benchmarking neural network robustness to common corruptions and perturbations. *Int. Conf. Learn. Represent.*, 2019.
- Dan Hendrycks, Steven Basart, Norman Mu, Saurav Kadavath, Frank Wang, Evan Dorundo, Rahul Desai, Tyler Zhu, Samyak Parajuli, Mike Guo, et al. The many faces of robustness: A critical analysis of out-of-distribution generalization. In *Int. Conf. Comput. Vis.*, 2021a.
- Dan Hendrycks, Kevin Zhao, Steven Basart, Jacob Steinhardt, and Dawn Song. Natural adversarial examples. In *IEEE Conf. Comput. Vis. Pattern Recog.*, 2021b.
- Geoffrey Hinton, Oriol Vinyals, and Jeff Dean. Distilling the knowledge in a neural network. *arXiv preprint arXiv:1503.02531*, 2015.
- Saihui Hou, Xinyu Pan, Chen Change Loy, Zilei Wang, and Dahua Lin. Learning a unified classifier incrementally via rebalancing. In *IEEE Conf. Comput. Vis. Pattern Recog.*, 2019.
- Neil Houlsby, Andrei Giurgiu, Stanislaw Jastrzebski, Bruna Morrone, Quentin De Laroussilhe, Andrea Gesmundo, Mona Attariyan, and Sylvain Gelly. Parameter-efficient transfer learning for nlp. In *Int. Conf. Mach. Lear.*, 2019a.
- Neil Houlsby, Andrei Giurgiu, Stanislaw Jastrzebski, Bruna Morrone, Quentin De Laroussilhe, Andrea Gesmundo, Mona Attariyan, and Sylvain Gelly. Parameter-efficient transfer learning for nlp. In *Int. Conf. Mach. Lear.*, 2019b.
- Paul Janson, Wenxuan Zhang, Rahaf Aljundi, and Mohamed Elhoseiny. A simple baseline that questions the use of pretrained-models in continual learning. In *NeurIPS Workshop on Distribution Shifts*, 2022.
- Menglin Jia, Luming Tang, Bor-Chun Chen, Claire Cardie, Serge J. Belongie, Bharath Hariharan, and Ser-Nam Lim. Visual prompt tuning. In *Eur. Conf. Comput. Vis.*, 2022.
- Dahyun Jung, Dongyoon Han, Jihwan Bang, and Hwanjun Song. Generating instance-level prompts for rehearsal-free continual learning. In *Int. Conf. Comput. Vis.*, 2023.
- Heechul Jung, Jeongwoo Ju, Minju Jung, and Junmo Kim. Less-forgetting learning in deep neural networks. *arXiv preprint arXiv:1607.00122*, 2016.
- James Kirkpatrick, Razvan Pascanu, Neil Rabinowitz, Joel Veness, Guillaume Desjardins, Andrei A Rusu, Kieran Milan, John Quan, Tiago Ramalho, Agnieszka Grabska-Barwinska, et al. Overcoming catastrophic forgetting in neural networks. *PNAS*, 114(13), 2017.
- Alex Krizhevsky, Geoffrey Hinton, et al. Learning multiple layers of features from tiny images, 2009.
- Solomon Kullback and Richard A Leibler. On information and sufficiency. *The annals of mathematical statistics*, 22 (1):79–86, 1951.
- Ananya Kumar, Aditi Raghunathan, Robbie Matthew Jones, Tengyu Ma, and Percy Liang. Fine-tuning can distort pretrained features and underperform out-of-distribution. In *Int. Conf. Learn. Represent.*, 2022.

- Janghyeon Lee, Hyeong Gwon Hong, Donggyu Joo, and Junmo Kim. Continual learning with extended kronecker-factored approximate curvature. In *IEEE Conf. Comput. Vis. Pattern Recog.*, 2020.
- Zhizhong Li and Derek Hoiem. Learning without forgetting. *IEEE Trans. Pattern Anal. Mach. Intell.*, 2017.
- Jian Liang, Ran He, and Tieniu Tan. A comprehensive survey on test-time adaptation under distribution shifts. *arXiv preprint arXiv:2303.15361*, 2023.
- Xialei Liu, Marc Masana, Luis Herranz, Joost Van de Weijer, Antonio M Lopez, and Andrew D Bagdanov. Rotate your networks: Better weight consolidation and less catastrophic forgetting. In *ICPR*, 2018.
- Yaoyao Liu, Yuting Su, An-An Liu, Bernt Schiele, and Qianru Sun. Mnemonics training: Multi-class incremental learning without forgetting. In *IEEE Conf. Comput. Vis. Pattern Recog.*, 2020.
- Yuejiang Liu, Parth Kothari, Bastien van Delft, Baptiste Bellot-Gurlet, Taylor Mordan, and Alexandre Alahi. Ttt++: When does self-supervised test-time training fail or thrive? *Adv. Neural Inform. Process. Syst.*, 2021.
- Amrutha Machireddy, Ranganath Krishnan, Nilesh Ahuja, and Omesh Tickoo. Continual active adaptation to evolving distributional shifts. In *Proceedings of the IEEE/CVF Conference on Computer Vision and Pattern Recognition*, pp. 3444–3450, 2022.
- Arun Mallya and Svetlana Lazebnik. Packnet: Adding multiple tasks to a single network by iterative pruning. In *IEEE Conf. Comput. Vis. Pattern Recog.*, 2018.
- Arun Mallya, Dillon Davis, and Svetlana Lazebnik. Piggyback: Adapting a single network to multiple tasks by learning to mask weights. In *Eur. Conf. Comput. Vis.*, 2018.
- Marc Masana, Xialei Liu, Bartłomiej Twardowski, Mikel Menta, Andrew D Bagdanov, and Joost van de Weijer. Class-incremental learning: survey and performance evaluation on image classification. *IEEE Trans. Pattern Anal. Mach. Intell.*, 2022.
- Mark D McDonnell, Dong Gong, Amin Parvaneh, Ehsan Abbasnejad, and Anton van den Hengel. Ranpac: Random projections and pre-trained models for continual learning. *Adv. Neural Inform. Process. Syst.*, 36, 2024.
- Thomas Mensink, Jakob Verbeek, Florent Perronnin, and Gabriela Csurka. Distance-based image classification: Generalizing to new classes at near-zero cost. *IEEE Trans. Pattern Anal. Mach. Intell.*, 2013.
- Martial Mermillod, Aurélie Bugaïska, and Patrick Bonin. The stability-plasticity dilemma: Investigating the continuum from catastrophic forgetting to age-limited learning effects. *Frontiers in psychology*, 4:504, 2013.
- Mohammad Hasanzadeh Mofrad, Rami Melhem, Yousuf Ahmad, and Mohammad Hammoud. Accelerating distributed inference of sparse deep neural networks via mitigating the straggler effect. In *2020 IEEE High Performance Extreme Computing Conference (HPEC)*, pp. 1–7, 2020. doi: 10.1109/HPEC43674.2020.9286189.
- Thaha Mohammed, Carlee Joe-Wong, Rohit Babbar, and Mario Di Francesco. Distributed inference acceleration with adaptive dnn partitioning and offloading. In *IEEE INFOCOM 2020 - IEEE Conference on Computer Communications*, 2020.
- Shuaicheng Niu, Jiaxiang Wu, Yifan Zhang, Yaofo Chen, Shijian Zheng, Peilin Zhao, and Minghui Tan. Efficient test-time model adaptation without forgetting. In *Int. Conf. Mach. Lear.*, volume 162 of *Proceedings of Machine Learning Research*. PMLR, 2022.
- Shuaicheng Niu, Jiaxiang Wu, Yifan Zhang, Zhiqian Wen, Yaofo Chen, Peilin Zhao, and Minghui Tan. Towards stable test-time adaptation in dynamic wild world. In *Int. Conf. Learn. Represent.*, 2023.
- Oleksiy Ostapenko, Mihai Puscas, Tassilo Klein, Patrick Jahnichen, and Moin Nabi. Learning to remember: A synaptic plasticity driven framework for continual learning. In *IEEE Conf. Comput. Vis. Pattern Recog.*, 2019.
- Aristeidis Panos, Yuriko Kobe, Daniel Olmeda Reino, Rahaf Aljundi, and Richard E Turner. First session adaptation: A strong replay-free baseline for class-incremental learning. In *Int. Conf. Comput. Vis.*, 2023.
- German I Parisi, Ronald Kemker, Jose L Part, Christopher Kanan, and Stefan Wermter. Continual lifelong learning with neural networks: A review. *Neural Networks*, 113, 2019.

- Xingchao Peng, Ben Usman, Neela Kaushik, Judy Hoffman, Dequan Wang, and Kate Saenko. Visda: The visual domain adaptation challenge. *arXiv preprint arXiv:1710.06924*, 2017.
- Ameya Prabhu, Philip HS Torr, and Puneet K Dokania. Gdumb: A simple approach that questions our progress in continual learning. In *Eur. Conf. Comput. Vis.*, 2020.
- Ameya Prabhu, Hasan Abed Al Kader Hammoud, Puneet K Dokania, Philip HS Torr, Ser-Nam Lim, Bernard Ghanem, and Adel Bibi. Computationally budgeted continual learning: What does matter? In *IEEE Conf. Comput. Vis. Pattern Recog.*, 2023.
- Joaquin Quinonero-Candela, Masashi Sugiyama, Anton Schwaighofer, and Neil D Lawrence. *Dataset shift in machine learning*. Mit Press, 2008.
- Alec Radford, Jong Wook Kim, Chris Hallacy, Aditya Ramesh, Gabriel Goh, Sandhini Agarwal, Girish Sastry, Amanda Askell, Pamela Mishkin, Jack Clark, et al. Learning transferable visual models from natural language supervision. In *Int. Conf. Mach. Lear.*, 2021.
- Sylvestre-Alvise Rebuffi, Alexander Kolesnikov, Georg Sperl, and Christoph H Lampert. icarl: Incremental classifier and representation learning. In *IEEE Conf. Comput. Vis. Pattern Recog.*, 2017.
- Tal Ridnik, Emanuel Ben-Baruch, Asaf Noy, and Lihi Zelnik-Manor. Imagenet-21k pretraining for the masses, 2021.
- Andrei A Rusu, Neil C Rabinowitz, Guillaume Desjardins, Hubert Soyer, James Kirkpatrick, Koray Kavukcuoglu, Razvan Pascanu, and Raia Hadsell. Progressive neural networks. *arXiv preprint arXiv:1606.04671*, 2016.
- Jonathan Schwarz, Wojciech Czarnecki, Jelen Luketina, Agnieszka Grabska-Barwinska, Yee Whye Teh, Razvan Pascanu, and Raia Hadsell. Progress & compress: A scalable framework for continual learning. In *Int. Conf. Mach. Lear.*, 2018.
- James Seale Smith, Leonid Karlinsky, Vyshnavi Gutta, Paola Cascante-Bonilla, Donghyun Kim, Assaf Arbelle, Rameswar Panda, Rogerio Feris, and Zsolt Kira. Coda-prompt: Continual decomposed attention-based prompting for rehearsal-free continual learning. *arXiv e-prints*, pp. arXiv–2211, 2022.
- Hanul Shin, Jung Kwon Lee, Jaehong Kim, and Jiwon Kim. Continual learning with deep generative replay. *Adv. Neural Inform. Process. Syst.*, 2017.
- James Seale Smith, Leonid Karlinsky, Vyshnavi Gutta, Paola Cascante-Bonilla, Donghyun Kim, Assaf Arbelle, Rameswar Panda, Rogerio Feris, and Zsolt Kira. Coda-prompt: Continual decomposed attention-based prompting for rehearsal-free continual learning. In *IEEE Conf. Comput. Vis. Pattern Recog.*, 2023.
- Junha Song, Jungsoo Lee, In So Kweon, and Sungha Choi. Ecotta: Memory-efficient continual test-time adaptation via self-distilled regularization. In *IEEE Conf. Comput. Vis. Pattern Recog.*, 2023.
- Hai-Long Sun, Da-Wei Zhou, Han-Jia Ye, and De-Chuan Zhan. Pilot: A pre-trained model-based continual learning toolbox. *arXiv preprint arXiv:2309.07117*, 2023.
- Yu Sun, Xiaolong Wang, Zhuang Liu, John Miller, Alexei Efros, and Moritz Hardt. Test-time training with self-supervision for generalization under distribution shifts. In *Int. Conf. Mach. Lear.*, 2020.
- Andrés Villa, Juan León Alcázar, Motasem Alfarra, Kumail Alhamoud, Julio Hurtado, Fabian Caba Heilbron, Alvaro Soto, and Bernard Ghanem. Pivot: Prompting for video continual learning. In *IEEE Conf. Comput. Vis. Pattern Recog.*, 2023.
- C. Wah, S. Branson, P. Welinder, P. Perona, and S. Belongie. The Caltech-UCSD Birds-200-2011 Dataset. Technical Report CNS-TR-2011-001, California Institute of Technology, 2011.
- Dequan Wang, Evan Shelhamer, Shaoteng Liu, Bruno Olshausen, and Trevor Darrell. Tent: Fully test-time adaptation by entropy minimization. In *Int. Conf. Learn. Represent.*, 2021.
- Liyuan Wang, Xingxing Zhang, Hang Su, and Jun Zhu. A comprehensive survey of continual learning: Theory, method and application, 2023a.
- Qin Wang, Olga Fink, Luc Van Gool, and Dengxin Dai. Continual test-time domain adaptation. In *IEEE Conf. Comput. Vis. Pattern Recog.*, 2022a.

- Shuai Wang, Daoan Zhang, Zipei Yan, Jianguo Zhang, and Rui Li. Feature alignment and uniformity for test time adaptation, 2023b.
- Yabin Wang, Zhiwu Huang, and Xiaopeng Hong. S-prompts learning with pre-trained transformers: An occam’s razor for domain incremental learning. *Adv. Neural Inform. Process. Syst.*, 35, 2022b.
- Zhenyi Wang, Li Shen, Donglin Zhan, Qiuling Suo, Yanjun Zhu, Tiehang Duan, and Mingchen Gao. Metamix: Towards corruption-robust continual learning with temporally self-adaptive data transformation. In *Proceedings of the IEEE/CVF Conference on Computer Vision and Pattern Recognition*, pp. 24521–24531, 2023c.
- Zifeng Wang, Zizhao Zhang, Sayna Ebrahimi, Ruoxi Sun, Han Zhang, Chen-Yu Lee, Xiaoqi Ren, Guolong Su, Vincent Perot, Jennifer Dy, et al. Dualprompt: Complementary prompting for rehearsal-free continual learning. In *Eur. Conf. Comput. Vis.*, 2022c.
- Zifeng Wang, Zizhao Zhang, Chen-Yu Lee, Han Zhang, Ruoxi Sun, Xiaoqi Ren, Guolong Su, Vincent Perot, Jennifer Dy, and Tomas Pfister. Learning to prompt for continual learning. In *IEEE Conf. Comput. Vis. Pattern Recog.*, 2022d.
- Ye Xiang, Ying Fu, Pan Ji, and Hua Huang. Incremental learning using conditional adversarial networks. In *Int. Conf. Comput. Vis.*, 2019.
- Friedemann Zenke, Ben Poole, and Surya Ganguli. Continual learning through synaptic intelligence. In *Int. Conf. Mach. Lear.*, 2017.
- Xiaohua Zhai, Joan Puigcerver, Alexander Kolesnikov, Pierre Ruysen, Carlos Riquelme, Mario Lucic, Josip Djolonga, Andre Susano Pinto, Maxim Neumann, Alexey Dosovitskiy, et al. A large-scale study of representation learning with the visual task adaptation benchmark. *arXiv preprint arXiv:1910.04867*, 2019.
- Gengwei Zhang, Liyuan Wang, Guoliang Kang, Ling Chen, and Yunchao Wei. Slca: Slow learner with classifier alignment for continual learning on a pre-trained model. In *Int. Conf. Comput. Vis.*, 2023.
- Marvin Mengxin Zhang, Sergey Levine, and Chelsea Finn. Memo: Test time robustness via adaptation and augmentation. In *NeurIPS 2021 Workshop on Distribution Shifts: Connecting Methods and Applications*, 2021.
- Yuanhan Zhang, Zhenfei Yin, Jing Shao, and Ziwei Liu. Benchmarking omni-vision representation through the lens of visual realms. In *Eur. Conf. Comput. Vis.* Springer, 2022.
- Hao Zhao, Yuejiang Liu, Alexandre Alahi, and Tao Lin. On pitfalls of test-time adaptation, 2023.
- Da-Wei Zhou, Han-Jia Ye, and De-Chuan Zhan. Co-transport for class-incremental learning. In *ACM MM*, 2021.
- Da-Wei Zhou, Zi-Wen Cai, Han-Jia Ye, De-Chuan Zhan, and Ziwei Liu. Revisiting class-incremental learning with pre-trained models: Generalizability and adaptivity are all you need. *Int. J. Comput. Vis.*, 2024a.
- Da-Wei Zhou, Hai-Long Sun, Han-Jia Ye, and De-Chuan Zhan. Expandable subspace ensemble for pre-trained model-based class-incremental learning. In *Int. Conf. Comput. Vis.*, 2024b.
- Kaiyang Zhou, Jingkang Yang, Chen Change Loy, and Ziwei Liu. Learning to prompt for vision-language models. *Int. Conf. Comput. Vis.*, 2022.

In this supplementary material, we provide more details about the experimental results mentioned in the main paper, as well as additional empirical evaluations and discussions. The supplementary material is organized as follows: In Section A, we provide more details about NCM. In Section C, we evaluate the effect of task order. In Section D, provide additional evaluations on CIFAR100-C dataset. In Section E, reports the full experimental results ablation studies in the main paper. In Section G, we analyze the inference cost of PLASTIC. In Section H, provides an ablation study about the Adapter size in PLASTIC. In Section I, we detail the baselines, and datasets used in our experiments.

A NCM WITH PTMS

Inspired by (Rebuffi et al., 2017; Mensink et al., 2013), we use a NCM approach to transfer PTM knowledge for incremental tasks. Let E_θ be the PTM model’s feature extractor. We compute class prototypes c_k for $k=1, \dots, K$ by averaging the embeddings of each class in the current task \mathcal{D}^t as:

$$c_k = \frac{1}{N_k} \sum_{j=1}^{|\mathcal{D}^t|} \delta_{y_j, k} E_\theta(\mathbf{x}_j), \quad (6)$$

where $\delta_{a,b}$ is the Kronecker delta. For a test instance \mathbf{x}_i , the class probability $p_\theta(y_i = k | \mathbf{z}_i)$ is computed using the dot product between the feature representation $\mathbf{z}_i = E_\theta(\mathbf{x}_i)$ and each prototype:

$$p_\theta(y_i = k | \mathbf{z}_i) = \frac{\exp(\mathbf{z}_i \cdot \mathbf{c}_k)}{\sum_j \exp(\mathbf{z}_i \cdot \mathbf{c}_j)}. \quad (7)$$

Our model f , combining E_θ and prototype classifiers, achieves competitive performance without fine-tuning (see Sec. 4.2). However, performance drops when downstream datasets exhibit domain shifts, especially with significant concept drift (Alfassy et al., 2022; Hendrycks et al., 2021b).

B COMPUTATIONAL ANALYSIS

Table 8 presents a comparative analysis of Class-Incremental Learning (CIL) methods across average accuracy, space complexity, and time complexity. PLASTIC (Ours) achieves the highest accuracy (83.36%), slightly outperforming EASE (83.32%) and RanPAC (82.69%).

Regarding space complexity, PLASTIC and RanPAC maintain constant scaling ($n + p$) for storage. These methods train only on the first task, requiring no additional parameters for subsequent tasks. In contrast, EASE, which trains an adapter for each task, scales linearly with the number of tasks ($n + p \cdot T$). This method necessitates concatenating adapters during inference to update prototypes, increasing computational overhead. SLCA updates all model parameters, resulting in space complexity of n .

In terms of time complexity, PLASTIC and RanPAC achieve task-independent training and inference complexities of $\mathcal{O}(1)$, making them computationally efficient. Sequentially updated methods like EASE, SLCA, and Finetune Adapter incur higher training time complexities ($\mathcal{O}(T)$) due to the need to process all tasks incrementally. EASE further incurs task-dependent inference complexity ($\mathcal{O}(T)$) due to the concatenation of task-specific adapters. The analysis provided here focuses on whether inference complexity scales with the number of tasks; task-specific analysis subject to TTA in our PLASTIC is detailed in Section G.

PLASTIC and RanPAC are parameter-efficient, introducing only 1–3% additional trainable parameters through adapters. In contrast, EASE requires 1–3% parameters per task, leading to a total proportional to the number of tasks. SLCA updates 100% of the model parameters, significantly increasing memory requirements.

PLASTIC’s combination of task-independent time complexity, constant space complexity, and high accuracy establishes it as a computationally and memory-efficient solution for CIL.

Table 8: Comparison of class-incremental learning (CIL) methods based on average accuracy, space complexity (storage), and time complexity (training and inference) as functions of the number of tasks T . n and p represent the number of model’s and adapter’s parameters, respectively. Space complexity (storage) indicates the network size growth with additional tasks. Time complexity measures the computational cost during training and inference. NCM does not require training, while EASE, SLCA, and Finetune Adapter train sequentially on all tasks. PLASTIC and RanPAC train only on the first task. PLASTIC achieves the highest average accuracy (83.36%) with constant space complexity $n + p$ and task-independent time complexity $\mathcal{O}(1)$.

	Methods	Trainable Param.	Space Complexity Storage	Time Complexity		Avg. Accuracy
				Training	Inference	
	NCM	0	n	–	$\mathcal{O}(1)$	77.33
Sequential Updating	Finetune Adapter	1–3%	$n + p$	$\mathcal{O}(T)$	$\mathcal{O}(1)$	54.87
	SLCA (Zhang et al., 2023)	100%	n	$\mathcal{O}(T)$	$\mathcal{O}(1)$	80.77
	EASE (Zhou et al., 2024b)	$1 - 3\% \times T$	$n + p \cdot T$	$\mathcal{O}(T)$	$\mathcal{O}(T)$	83.32
First Session Adaptation	ADAM (Zhou et al., 2024a)	1–3%	$n + p$	$\mathcal{O}(1)$	$\mathcal{O}(1)$	80.02
	RanPAC (McDonnell et al., 2024)	1–3%	$n + p$	$\mathcal{O}(1)$	$\mathcal{O}(1)$	82.69
	PLASTIC (Ours)	1–3%	$n + p$	$\mathcal{O}(1)$	$\mathcal{O}(1)$	83.36

C EFFECT OF VARYING TASK SEQUENCE ORDERS

This section evaluates the adaptability of our proposed method PLASTIC and compares it with ADAM in CIL scenarios on the 5-Datasets benchmark. We specifically delve deeper into the experiments discussed in Sec. 4.3 of the main paper, where we analyze the influence of task order. on the impact of the task order. We provide more detailed experimental results considering multiple task orders. The task sequences include variations with SVHN, MNIST, CIFAR10, NotMNIST, and FashionMNIST. Results are reported in Tab. 9. The orange cells corresponding to the first task, both ADAM and PLASTIC have been trained on.

The results indicate the substantial influence of task sequence on model performance, highlighting the pivotal role of the initial task. PLASTIC consistently surpasses ADAM in all sequences, with a maximum performance gain of +10.29% observed in the SVHN \rightarrow MNIST \rightarrow CIFAR10 \rightarrow NotMNIST \rightarrow FashionMNIST sequence. This suggests that PLASTIC effectively leverages unlabeled data from subsequent tasks to improve its adaptability.

Table 9: Performance Comparison of ADAM and PLASTIC Across Varying Task Sequence Orders in Class-Incremental Learning. Top-1 accuracy is reported (\uparrow). Orange cells indicate the task that the model has been trained on. Model used in ViT-B/16 pre-trained on Imagenet-21K.

Method		SVHN	MNIST	CIFAR10	NotMNIST	FashionMNIST	Average
NCM		33.18	83.78	95.63	68.85	83.18	72.92
ADAM (Zhou et al., 2024a)	SVHN	33.44	83.84	95.62	68.85	83.14	72.98
	MNIST	92.44	93.95	72.77	83.00	40.22	76.48
	CIFAR10	97.24	67.97	83.63	31.33	84.04	72.84
	NotMNIST	71.02	83.66	38.20	86.51	95.89	75.06
	FashionMNIST	84.19	31.52	85.69	95.96	69.93	73.46
Ours	SVHN	95.13	96.48	67.33	78.43	78.96	83.27
	MNIST	97.89	76.15	82.35	83.09	53.28	78.55
	CIFAR10	98.95	70.37	83.24	35.03	82.19	73.96
	NotMNIST	88.67	83.82	59.16	92.76	73.61	79.60
	FashionMNIST	91.02	44.35	84.63	82.50	77.78	76.06

D EVALUATION ON CIFAR100-C WITH LEVEL-5 CORRUPTIONS

We compare our method, PLASTIC, with state-of-the-art methods on CIFAR100-C with Level-5 corruptions (?), as summarized in Tab. 10. The NCM performs poorly, yielding a 53.89% average accuracy, due to its reliance on pre-trained representations. ADAM improves upon this with a 66.57% average accuracy, courtesy of its initial task training.

In contrast, PLASTIC achieves the highest average accuracy of 68.00%, outperforming ADAM by a significant margin of +5.13% on CIFAR100-C. These results substantiate PLASTIC’s superior adaptability and robustness to a variety of corruptions.

Table 10: Average and last performance comparison on seven datasets with **ViT-B/16-IN21K** as the backbone on *CIFAR100-C* with Level-5 corruptions (Hendrycks & Dietterich, 2019). The best performance is shown in bold, and the second-best is underlined.

Method	Noise			Defoc.	Blur			Snow	Weather			Brit.	Average
	Gauss.	Shot	Impul.		Glass	Motion	Zoom		Frost	Fog			
NCM	35.52	39.05	46.89	59.78	31.29	56.99	65.04	64.41	63.99	50.13	79.68	53.89	
ADAM (Zhou et al., 2024a)	37.52	48.73	65.03	78.02	39.80	74.59	79.27	76.92	73.34	70.50	88.59	<u>66.57</u>	
PLASTIC	47.33	51.45	67.89	78.52	42.70	75.00	79.00	75.31	72.49	69.20	89.09	68.00	

E ABLATION STUDY: AUGMENTATIONS, ITERATIONS, AND BATCH SIZE

This section provides the additional ablation studies on the effect of augmentations M , iterations N , and batch size B .

Effect of adaptation augmentations M . This section investigates the impact of varying the number of augmentations M used during Phase II, as summarized in Tab. 11. Our method, PLASTIC, demonstrates robust performance across both VTAB and Imagenet-R datasets, irrespective of the number of augmentations. However, increasing M incurs computational costs during inference without a proportional performance gain. Thus, for efficiency, we recommend limiting augmentations to a small range $M \in [1, \dots, 8]$.

Table 11: Summarized results for VTAB and Imagenet-R datasets based on the number of augmentations M . (Mean \pm Std. Dev.)

Augmentations (M)	VTAB \uparrow	Imagenet-R \uparrow
4	90.14 \pm 0.72	75.30 \pm 0.87
8	<u>90.55 \pm 0.61</u>	75.22 \pm 0.91
16	90.67 \pm 0.39	75.26 \pm 0.85
24	90.52 \pm 0.36	<u>75.23 \pm 0.80</u>

Effect of adaptation iterations N . Tab. 12 summarizes the impact of increasing test-time iterations. Performance degrades as N increases across both datasets. Specifically, VTAB accuracy drops from 91.28% with one iteration to 80.78% at four iterations, while Imagenet-R follows a similar trend, declining from 76.88% to 69.13%. These results indicate that excessive test-time adaptation may lead to overfitting or instability.

Table 12: Impact of adaptation iterations N .

Iterations	VTAB (\bar{A}) \uparrow	Imagenet-R (\bar{A}) \uparrow
$N = 1$	91.28 \pm 0.64	76.88 \pm 1.02
$N = 2$	<u>87.34 \pm 3.05</u>	<u>74.77 \pm 1.22</u>
$N = 3$	84.07 \pm 3.53	70.14 \pm 3.35
$N = 4$	80.78 \pm 5.45	69.13 \pm 2.08

Effect of Batch-size B . Tab. 13 reports the impact of batch size B on performance. For VTAB, accuracy stabilizes around 90% for $B \geq 4$, with minimal gains from further increases. Conversely, Imagenet-R shows a decline in performance as B increases, suggesting that a mix of low- and high-entropy samples may negatively impact the TTA process (Niu et al., 2022).

Table 13: Impact of batch size B on VTAB and ImageNet-R performance in PLASTIC. Results are reported as mean \pm standard deviation.

Batch Size (B)	VTAB \uparrow	Imagenet-R \uparrow
1	88.14 \pm 1.71	79.11 \pm 1.46
4	89.81 \pm 2.62	<u>78.22 \pm 2.54</u>
8	88.91 \pm 2.87	76.62 \pm 1.93
16	91.28 \pm 0.64	76.88 \pm 1.02
32	<u>90.31 \pm 0.09</u>	69.12 \pm 0.60

F DATA EFFICIENCY

This section presents the results of the ablation study conducted in Sec.4.3 of the main paper, which focuses on the data efficiency of our method PLASTIC. Tab. 15 details the results presented in Fig. 4 in the main paper.

Method	CUB-Inc10		IN-R-Inc5	
	FWT	BWT	FWT	BWT
ADAM (Zhou et al., 2024a)	-0.47	-4.64	-1.68	-11.96
RanPAC (McDonnell et al., 2024)	-0.24	-2.99	-0.78	-10.92
PLASTIC (Ours)	2.29	-1.92	-0.21	-10.65

Table 14: Comparison of forward transfer (FTW) and backward transfer (BWT) on CUB and ImageNet-R across different baselines.

Table 15: Performance comparison under varying data scarcity for training.

Training Data (%)	NCM		ADAM		PLASTIC (Ours)	
	VTAB	Imagenet-R	VTAB	Imagenet-R	VTAB	Imagenet-R
20%	87.52 \pm 0.91	56.27 \pm 0.45	87.49 \pm 0.91	56.75 \pm 0.40	88.00 \pm 0.03	57.39 \pm 0.29
40%	88.84 \pm 0.76	59.41 \pm 1.42	88.78 \pm 0.66	63.34 \pm 1.51	89.57 \pm 0.88	65.66 \pm 1.15
60%	89.51 \pm 0.69	60.82 \pm 1.10	89.56 \pm 0.71	68.67 \pm 1.08	90.29 \pm 0.14	70.89 \pm 1.09
80%	89.43 \pm 0.90	61.18 \pm 1.32	89.61 \pm 0.75	72.05 \pm 0.82	90.38 \pm 0.24	73.98 \pm 0.75
100%	89.74 \pm 0.78	61.93 \pm 1.49	89.90 \pm 0.67	73.59 \pm 1.34	90.54 \pm 0.64	75.24 \pm 0.91

The study aims to examine how well PLASTIC performs under varying degrees of data scarcity for training. We compare PLASTIC’s performance against state-of-the-art methods like NCM and ADAM across different datasets including VTAB and Imagenet-R.

G INFERENCE COST

Inference Cost Analysis. PLASTIC introduces additional computation through an optimization step before prediction. We analyze its inference cost by comparing the inference time of PLASTIC with ADAM and NCM. Specifically, inference time in PLASTIC includes both TTA optimization and final prediction. Tab. 16 reports the average inference time (ms) over five runs on an A100 (48GB) GPU, using one iteration ($N = 1$) and $M = 8$ augmentations.

The computational overhead in PLASTIC is a trade-off for improved plasticity and robustness. However, this cost is mitigated by its efficiency during training, where only Layer Normalization parameters are updated in the initial task.

Table 16: Inference Time Comparison (ms). Results are averaged over 5 runs. GFLOPS/GMACs are evaluated at batch size $B = 16$.

Batch Size	PLASTIC	NCM	ADAM
B=16	1820	22	27
GFLOPS	85.45	33.72	<u>34.18</u>
GMACs	42.73	16.86	<u>17.09</u>

Execution Time Analysis. Tab. 17 quantifies PLASTIC’s inference time across varying batch sizes B and adaptation iterations N , highlighting computational trade-offs. Notably, execution time scales more gradually with larger batch sizes.

For instance, increasing from $B = 1$ to $B = 4$ at $N = 1$ raises inference time by 280 ms (from 190 ms to 470 ms). However, when increasing from $B = 8$ to $B = 16$, execution time rises by only 770 ms (from 1000 ms to 1770 ms). This suggests that PLASTIC achieves a form of computational efficiency with larger batch sizes, reducing execution time per unit increase in batch size.

Table 17: Execution Time Comparison (ms) for varying batch size B and adaptation iterations N .

		Iterations			
		N=1	N=2	N=3	N=4
Batch-size	B=1	190	<u>250</u>	320	340
	B=4	470	630	680	810
	B=8	1000	1110	1270	1410
	B=16	1770	2140	2480	2460

H ADAPTER

The Adapter module, a bottleneck structure extensively studied in prior works (Chen et al., 2022b; Houlsby et al., 2019a), enables fine-tuning of Vision Transformer (ViT) outputs. Composed of a down-projection $W_{\text{down}} \in \mathbb{R}^{d \times r}$, a non-linear activation function, and an up-projection $W_{\text{up}} \in \mathbb{R}^{r \times d}$, it facilitates dimensionality reduction and subsequent restoration. We adopt the AdaptMLP structure as introduced in AdaptFormer (Chen et al., 2022b), effectively replacing ViT’s native MLP. Given the input \mathbf{x}_ℓ to the MLP, the output can be expressed as:

$$\text{MLP}(\mathbf{x}_\ell) + s \cdot \text{ReLU}(\mathbf{x}_\ell W_{\text{down}}) W_{\text{up}}, \quad (8)$$

where s is an optional, learnable scaling parameter. As done in ADAM (Zhou et al., 2024a), during the adaptation phase, only adapter parameters are optimized, while the pre-trained weights of ViT remain fixed. We employ a hidden dimension r of 16, resulting in approximately 0.3 million tunable parameters, a figure substantially lower than the 86 million parameters in the standard ViT-B/16 model.

Ablation Study on Adapter Sizes in PLASTIC. Tab. 18 presents an ablation study examining the effect of varying adapter sizes r on the average performance across multiple datasets such as VTAB, CIFAR100, and ImageNet-R. The reported trainable parameters also scale with the adapter size, giving us an insight into the computational cost involved.

The table reveals that increasing the adapter size does not substantially improve the model’s performance. For instance, while moving from $r = 16$ to $r = 256$, the average accuracy on the VTAB dataset slightly decreases from 89.65% to 88.65%. A similar trend is observed in the CIFAR100 and ImageNet-R datasets, with only marginal performance improvements or even slight deteriorations.

More importantly, the increase in adapter size comes at a substantial computational cost. The number of trainable parameters rises exponentially with the adapter size, going from 0.30 Million for $r = 16$ to 4.73M for $r = 256$. This not only increases the model’s complexity but also makes it computationally expensive to train.

In summary, our analysis underscores the conclusion that while increasing the adapter size in PLASTIC may seem like a plausible avenue for performance improvement, it does not offer significant gains. Instead, it introduces computational inefficiencies due to the escalated number of trainable parameters, thereby questioning the trade-off between performance and computational cost.

Table 18: Comparison of PLASTIC Average performance Across Different Adapter Sizes r across datasets. Reported number of trainable parameters is in Million (M).

	$r = 16$	$r = 32$	$r = 128$	$r = 256$
Params (M)	0.30	0.60	2.37	4.73
VTAB	91.57	89.18	88.83	88.65
CIFAR100	92.34	90.14	89.25	89.04
ImageNet-R	76.88	75.03	<u>75.39</u>	74.99

I BASELINES

We briefly outline the methods against which our approach is evaluated:

- **Finetune:** Incrementally trains on new datasets, inducing catastrophic forgetting as a consequence.
- **Finetune Adapter (Chen et al., 2022b):** Retains pre-trained weights while optimizing an adapter module. Classifiers specific to the current dataset \mathbf{D}_t are fine-tuned, while those for previous classes are held constant.
- **LwF (Li & Hoiem, 2017):** Employs knowledge distillation (Hinton et al., 2015) as a regularizer to mitigate forgetting, relying on the legacy model for soft target generation.
- **L2P (Wang et al., 2022d):** A leading PTM-based CIL method that maintains a frozen pre-trained model while optimizing a prompt pool. It incorporates a ‘key-value’ pairing mechanism for prompt selection and leverages an auxiliary pre-trained model for prompt retrieval.
- **DualPrompt (Wang et al., 2022c):** An extension of L2P that utilizes two categories of prompts—general and expert—for enhanced performance. It also uses an additional pre-trained model for prompt retrieval.
- **ADAM (Zhou et al., 2024a):** fine-tunes the adapters (Chen et al., 2022b) only on the first task, among the sequences of all the tasks in a dataset, to adapt to the dataset at hand.

- **RanPAC** (McDonnell et al., 2024): uses random projection layers with pre-trained models to effectively prevent catastrophic forgetting without requiring rehearsal memory.
- **FeCAM** (Goswami et al., 2023): presents an exemplar-free continual learning method that uses a Bayes classifier with anisotropic Mahalanobis distance to model heterogeneous class distributions.
- **SLCA** (Zhang et al., 2023): improves the classification layer by modeling the class-wise distributions and aligning the classification layers in a post-hoc fashion.
- **EASE** (Zhou et al., 2024b): improves the classification layer by modeling the class-wise distributions and aligning the classification layers in a post-hoc fashion.

J DATASETS

We describe the datasets utilized in our study, summarized in Tab. 19. While CIFAR100, CUB200, and ImageNet-R are established CIL benchmarks (Rebuffi et al., 2017; Wang et al., 2022c; Zhou et al., 2021), ImageNet is ill-suited for PTM-based CIL evaluation due to data overlap (Wang et al., 2022d). Consequently, we introduce four additional benchmarks characterized by non-overlap with ImageNet, substantial domain diversity, and large-scale, cross-domain instances.

- **CIFAR100** (Krizhevsky et al., 2009): Comprises 100 classes, 60,000 images—50,000 for training and 10,000 for testing.
- **CUB200** (Wah et al., 2011): Focuses on fine-grained visual categorization, containing 11,788 bird images across 200 subcategories, with 9,430 for training and 2,358 for testing.
- **ImageNet-R** (Hendrycks et al., 2021a): Extended for CIL by (Wang et al., 2022c), includes various styles and hard instances, totaling 24,000 training and 6,000 testing instances.
- **ImageNet-A** (Hendrycks et al., 2021b): Features real-world adversarially filtered images, with 5,981 training and 1,519 testing instances.
- **OmniBenchmark** (Zhang et al., 2022): A diverse benchmark challenging PTM generalization, containing 89,697 training and 5,985 testing instances across multiple semantic realms.
- **VTAB** (Zhai et al., 2019): Encompasses 19 tasks across three categories—Natural, Specialized, and Structured. We select five datasets to construct a cross-domain CIL setting. Similar to ADAM (Zhou et al., 2024a), we select 5 to construct a cross-domain class-incremental learning setting, i.e., Resisc45, DTD, Pets, EuroSAT, and Flowers.
- **5-datasets** (Ebrahimi et al., 2020): a sequence of classification datasets including SVHN, CIFAR10, not-MNIST, Fashion-MNIST and, and MNIST.

Table 19: Introduction about benchmark datasets. ObjectNet, OmniBenchmark, and VTAB contain massive classes, and we sample a subset from them to construct the incremental learning task.

Dataset	# training instances	# testing instances	# Classes	Link
CIFAR100	50,000	10,000	100	Link
CUB200	9,430	2,358	200	Link
ImageNet-R	24,000	6,000	200	Link
ImageNet-A	5,981	1,519	200	Link
ObjectNet	26,509	6,628	200	Link
OmniBenchmark	89,697	5,985	300	Link
VTAB	1,796	8,619	50	Link
5-datasets	180,869	506,906	50	Link